Multigap nodeless superconductivity in the topological semimetal PdTe

Chengcheng Zhao,[1,2] Xiangqi Liu,[3] Jinjin Wang,[4] Chunqiang Xu,[5] Baomin Wang,[5] Wei Xia,[3,6] Zhenhai Yu,[3] Xiaobo Jin,[1] Xu Zhang,[1] Jing Wang,[1] Dongzhe Dai,[1] Chengpeng Tu,[1] Jiaying Nie,[1] Hanru Wang,[1] Yihan Jiao,[1] Daniel Duong,[7] Silu Huang,[7] Rongying Jin,[7] Zhu'an Xu,[4,8,9,*] Yanfeng Guo,[3,6,†] Xiaofeng Xu,[10,‡] and Shiyan Li[1,2,11,§]

[1]*State Key Laboratory of Surface Physics, Department of Physics, and Laboratory of Advanced Materials, Fudan University, Shanghai 200438, China*
[2]*Shanghai Research Center for Quantum Sciences, Shanghai 201315, China*
[3]*School of Physical Science and Technology, ShanghaiTech University, Shanghai 201210, China*
[4]*School of Physics, Zhejiang University, Hangzhou 310058, China*
[5]*School of Physical Science and Technology, Ningbo University, Ningbo 315211, China*
[6]*ShanghaiTech Laboratory for Topological Physics, Shanghai 201210, China*
[7]*SmartState Center for Experimental Nanoscale Physics, Department of Physics and Astronomy, University of South Carolina, Columbia, South Carolina 29208, USA*
[8]*State Key Laboratory of Silicon and Advanced Semiconductor Materials, Zhejiang University, Hangzhou 310027, China*
[9]*Hefei National Laboratory, Hefei 230088, China*
[10]*Department of Applied Physics, Zhejiang University of Technology, Hangzhou 310023, China*
[11]*Collaborative Innovation Center of Advanced Microstructures, Nanjing 210093, China*

(Received 12 October 2023; revised 1 March 2024; accepted 10 April 2024; published 2 May 2024)

Recently, PdTe was identified as a spin-orbit-coupled topological Dirac semimetal and was claimed to exhibit both bulk-nodal and surface-nodeless superconducting gaps. Here we report on ultra-low-temperature thermal-conductivity measurements on PdTe single crystals with $T_c = 4.5$ K to investigate its superconducting gap structure. It is found that the residual linear term κ_0/T is negligible in zero magnetic field. Furthermore, the field dependence of $\kappa_0(H)/T$ exhibits an S-shaped curve. These results suggest that PdTe has multiple nodeless superconducting gaps, which is at odds with the claimed bulk-nodal gap. The reason for the discrepancy is likely that previous angle-resolved photoemission spectroscopy measurements were only performed down to 2 K and cannot observe the smaller nodeless gap. The fully gapped superconducting state in PdTe is compatible with it being a topological superconductor candidate.

DOI: 10.1103/PhysRevB.109.174502

I. INTRODUCTION

The exploration of superconductors and their superconducting mechanisms is an important frontier of condensed-matter physics. High-temperature superconductors, unconventional superconductors, and topological superconductors are the novel ones that are attracting great attention. The pairing mechanism in unconventional superconductors is not phonon mediated, and the superconducting gap usually manifests the node (gap zero) [1]. Superconductors with topological band structure bring the idea of topological superconductors (TSCs), which are a source of Majorana fermions and hold potential applications in quantum computing [2]. In many cases, these three types of superconductors entangle with each other. For example, high-temperature iron-based superconductors are believed to be unconventional [3], and some of them are topological [4–7]. The excitation spectrum of a half-quantum vortex in a *p*-wave superconductor, theoretically predicted to feature a zero-energy Majorana fermion [8], has been exemplified by UTe_2 [9], yet the experimental status remains inconclusive [10–12]. There are still considerable controversies about those topological superconductor candidates [5,13–17].

PdTe crystallizes in the NiAs-type hexagonal structure with the space group $P6_3/\mathrm{mmc}$, as shown in Fig. 1(a), and has cell parameters $a = b = 4.152$ Å and $c = 5.671$ Å [18]. It exhibits a superconducting transition temperature (T_c) of approximately 4.5 K [18,19]. While there remains a debate on whether PdTe is a strongly coupled superconductor or not, there is no doubt that PdTe is a type-II superconductor [18,20]. During the exploration of iron-based high-temperature superconductors, PdTe was regarded as a distorted structure resulting from the sliding of anion and cation layers in iron chalcogenides and was investigated to get a clue as to the pairing mechanism of iron-based superconductors [21–23]. In contrast to iron chalcogenides, PdTe exhibits robust covalent bonding, negligible electron correlation, and orbital nondegeneracy, thus tending toward being a conventional superconductor [21–23].

*zhuan@zju.edu.cn
†guoyf@shanghaitech.edu.cn
‡xuxiaofeng@zjut.edu.cn
§shiyan_li@fudan.edu.cn

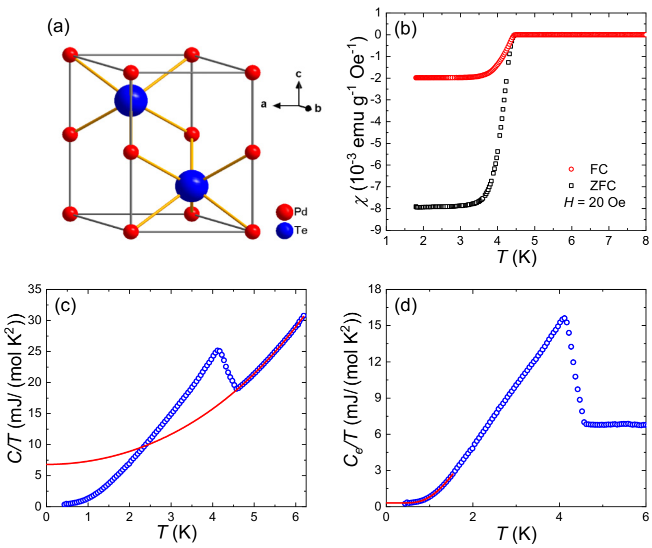

FIG. 1. (a) Crystal structure of PdTe. The Pd, Te atoms are presented as red and blue balls, respectively. (b) Low-temperature magnetization of a PdTe single crystal at $H = 20$ Oe, with zero-field-cooled (ZFC) and field-cooled (FC) processes, respectively. (c) Low-temperature specific heat for PdTe, plotted as the C/T vs T. The red line is a polynomial fit of the data between 4.62 and 6.19 K. (d) Electronic specific heat C_e obtained from $C_e = C - \alpha T^3 - \beta T^5$, plotted as the C_e/T vs T. The red line represents a fit of the data below 1.5 K to $C_e/T = \gamma_r + A\exp(-\Delta/kT)$.

However, recent angle-resolved photoemission spectroscopy (ARPES) study has revealed intriguing properties of PdTe, establishing it as a spin-orbit-coupled Dirac semimetal with a topological Fermi arc across the Fermi surface [24]. More interestingly, ARPES measurements have identified bulk-nodal and surface-nodeless superconducting gaps in PdTe [24]. The subsequent specific heat measurements show that the electronic specific heat C_e initially decreases in T^3 behavior, aligning with the characteristics of point nodes, and PdTe is suggested as an unconventional superconductor [25]. In this context more experimental studies are highly desired to clarify the superconducting gap structure of PdTe.

Ultra-low-temperature thermal transport represents a well-established bulk technique for investigating the energy gap of superconductors [26]. The existence of a finite residual linear term κ_0/T in zero magnetic field is clear evidence for gap nodes [26]. Moreover, the field dependence of κ_0/T may provide further information on the gap anisotropy, gap nodes, or multiple gaps [26].

In this article we present the ultra-low-temperature thermal-conductivity measurements on PdTe single crystal. A negligible κ_0/T in zero field and an S-shaped curve of $\kappa_0(H)/T$ are observed. These results suggest multiple nodeless superconducting gaps in PdTe. The reason for the discrepancy between our results and previous ARPES data is discussed.

II. EXPERIMENT

Single crystals of PdTe were grown using the method described in Ref. [18]. The single crystals are stable in air. DC magnetization measurement was performed in a magnetic property measurement system (MPMS, Quantum Design). The specific heat was measured in a physical property measurement system (PPMS-9, Quantum Design) via the relaxation method. A piece of PdTe single crystal was cut into a rectangular shape with dimensions 1.39 × 0.129 × 0.071 mm^3. Four silver wires were attached to the sample with silver paint, which were used for both resistivity and thermal-conductivity measurements. The low-temperature resistivity was measured in a ^{3}He cryostat. The thermal conductivity was measured in a dilution refrigerator by using a standard four-wire steady-state method with two RuO_2 chip thermometers, calibrated *in situ* against a reference RuO_2 thermometer. To ensure a homogeneous field distribution in the sample, all fields for resistivity and thermal-conductivity measurements were applied at a temperature above T_c.

III. RESULTS AND DISCUSSION

The temperature dependence of the magnetic susceptibility from 1.8 to 8 K at 20 Oe with both zero-field-cooled (ZFC) and field-cooled (FC) processes is plotted in Fig. 1(b), showing the onset of the superconductivity at 4.5 K, in agreement with previous reports [18,19,24,25]. Figure 1(c) shows the temperature dependence of the specific heat $C(T)$ in the low-T regime, plotted as C/T vs T. Above T_c, from 4.62 to 6.19 K, the C/T vs T is well fitted by the formula $C/T = \gamma_n + \alpha T^2 + \beta T^4$. The electronic specific heat coefficient γ_n and the phononic coefficients α and β are determined to be 6.81 mJ K^{-2} mol^{-1}, 0.51 mJ K^{-4} mol^{-1}, and 0.0028 mJ K^{-6} mol^{-1}, respectively. The electronic specific heat $C_e = C - \alpha T^3 - \beta T^5$ is shown in Fig. 1(d), plotted as C_e/T vs T. Below 1.5 K, C_e/T shows an exponential T dependence and can be well fitted by the formula $C_e/T = \gamma_r + A\exp(-\Delta/kT)$, with the energy gap $\Delta = 0.387$ meV and a finite residual linear term $\gamma_r = 0.31$ mJ K^{-2} mol^{-1}. The gap value is comparable to that obtained in Refs. [18,25], but our γ_r is smaller.

Figure 2(a) depicts the low-temperature resistivity behavior of a PdTe single crystal in magnetic fields up to 0.5 T. The normal-state resistivity shows a very weak temperature dependence below 8 K. The superconducting transition is very sharp in zero field, and the transition is gradually suppressed to lower temperatures with increasing the field. In order to estimate the zero-temperature upper critical field $\mu_0 H_{c2}(0)$, the temperature dependence of $\mu_0 H_{c2}$(T) is plotted in Fig. 2(b), defined by $\rho = 0$ in Fig. 2(a). By fitting the data using the Ginzburg-Landau equation $H_{c2}(T) = H_{c2}(0)[1 - (T/T_c)^2]/[1 + (T/T_c)^2]$ [27,28], $\mu_0 H_{c2}(0) \approx 0.23$ T is roughly estimated.

Figure 3 shows the temperature dependence of the thermal conductivity of PdTe single crystal under zero and various magnetic fields, plotted as κ/T vs T. The measured thermal conductivity contains two contributions, $\kappa = \kappa_e + \kappa_p$, which come from electrons and phonons, respectively. In order to separate the two contributions, the thermal conductivity in zero field is fitted to $\kappa/T = a + bT^{\alpha-1}$ [29,30]. The two terms aT and bT^α represent contributions from electrons and phonons, respectively. The residual linear term $\kappa_0/T \equiv a$ is obtained by extrapolating κ/T to $T = 0$ K. The power α

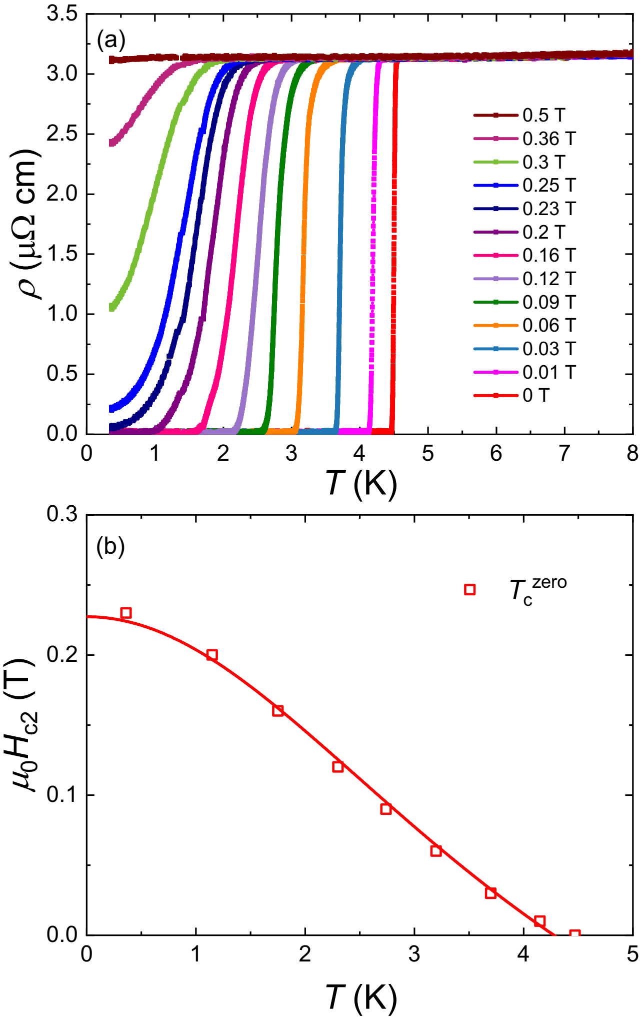

FIG. 2. (a) Low-temperature resistivity of a PdTe single crystal in magnetic fields up to 0.5 T. (b) Temperature dependence of the upper critical field $\mu_0 H_{c2}$, extracted from the T_c^{zero} values in panel (a). The red line is a fit to the Ginzburg-Landau equation $H_{c2}(T) = H_{c2}(0)[1-(T/T_c)^2]/[1+(T/T_c)^2]$, from which $\mu_0 H_{c2} \approx 0.23$ T is roughly estimated.

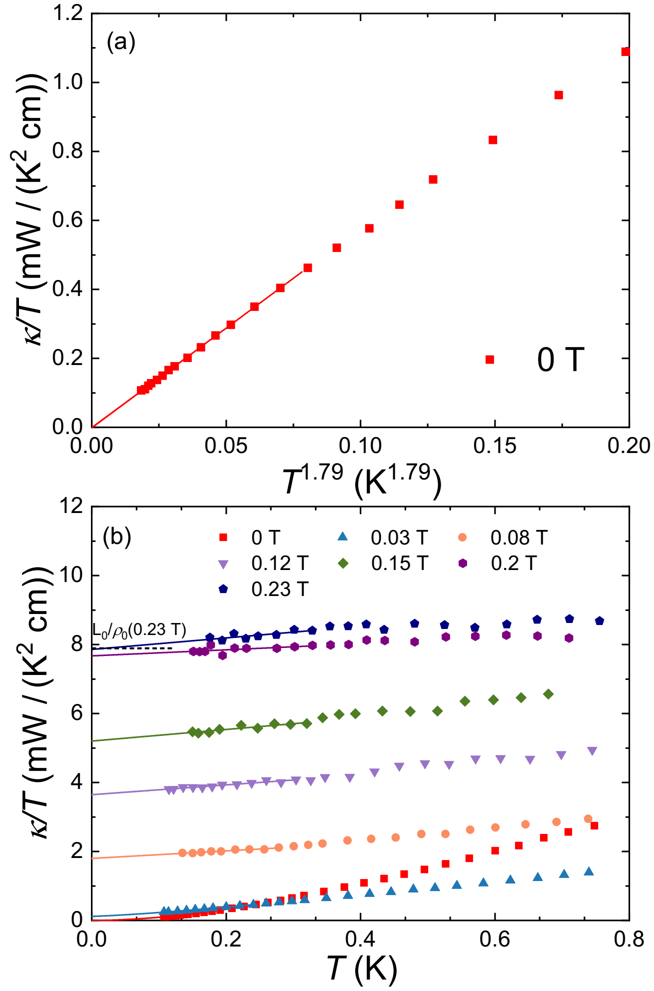

FIG. 3. (a) Temperature dependence of the thermal conductivity for the PdTe single crystal in zero field. The solid line represents a fit to $\kappa/T = a + bT^{\alpha-1}$, which gives a negligible residual linear term $\kappa_0/T = -1.7 \pm 0.5$ μW K^{-2} cm^{-1}. (b) Low-temperature thermal conductivity of the PdTe single crystal in magnetic fields up to 0.23 T. The dashed line is the normal-state Wiedemann-Franz law expectation $L_0/\rho_0(0.23\ T)$, with the Lorenz number $L_0 = 2.45 \times 10^{-8}$ W Ω K^{-2} and $\rho_0(0.23\ T) = 3.11$ μΩ cm.

is typically between 2 and 3, due to specular reflections of phonons at the sample boundary [29,30].

In zero field, the fitting results yield $\kappa_0/T = -1.7 \pm 0.5$ μW K^{-2} cm^{-1} and $\alpha = 2.79 \pm 0.04$. Considering our experimental error bar of ± 5 μW K^{-2} cm^{-1}, the κ_0/T of PdTe in zero field is essentially zero. For *s*-wave nodeless superconductors, there are no fermionic quasiparticles to conduct heat as $T \rightarrow 0$ K, since the Fermi surface is entirely gapped [29,30]. Consequently, the absence of a residual linear term κ_0/T should be observed, as seen in InBi and $NbSe_2$ [31,32]. However, for nodal superconductors, a substantial κ_0/T in zero field contributed by the nodal quasiparticles can be found [26]. For example, κ_0/T of the overdoped (T_c = 15 K) *d*-wave cuprate superconductor $Tl_2Ba_2CuO_{6+\delta}$ (Tl-2201) is 1.41 mW K^{-2} cm^{-1}, which is about 36% of the normal-state value κ_{N0}/T [33]. Therefore, the negligible κ_0/T of PdTe strongly indicates a bulk nodeless superconducting gap.

Given $\mu_0 H_{c2}(0) \approx 0.23$ T, the fitting of the normal-state data in 0.23 T results in $\kappa_0/T = 7.86 \pm 0.25$ mW K^{-2} cm^{-1}. This value of κ_0/T agrees well with the normal-state Wiedemann-Franz law expectation $L_0/\rho_0(0.23\ T) = 7.88$ mW K^{-2} cm^{-1}, with the Lorenz number $L_0 = 2.45 \times 10^{-8}$ W Ω K^{-2} and $\rho_0(0.23\ T) = 3.11$ μΩ cm. The validation of the Wiedemann-Franz law in the normal state substantiates the reliability of our thermal-conductivity measurements.

The field dependence of κ_0/T can offer additional insights into the structure of the superconducting gap [26]. In Fig. 3(b) the data in $\mu_0 H = 0.03$ T is also fitted to $\kappa/T = a + bT^{\alpha-1}$, which gives $\kappa_0/T = 0.118 \pm 0.019$ mW K^{-2} cm^{-1} and $\alpha = 2.27 \pm 0.12$. For magnetic fields of 0.08 T and above, the low-temperature part of the curves is quite straight; therefore we fit the data by fixing $\alpha = 2$. The variation of α with field suggests that the scattering of phonons by electrons in the vortex state becomes more and more dominant, which

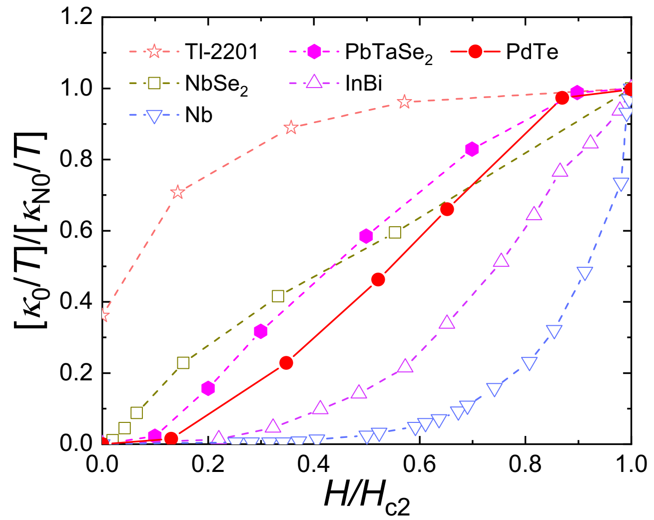

FIG. 4. Normalized residual linear term κ_0/T of PdTe as a function of H/H_{c2}. Similar data of the clean s-wave superconductor Nb [35], the dirty s-wave superconducting alloy InBi [31], the multiband s-wave superconductor $NbSe_2$ [32] and $PbTaSe_2$ [36], and an overdoped d-wave cuprate superconductor Tl-2201 [33] are shown for comparison.

results in a T^2 dependence of phonon thermal conductivity [34]. The normalized κ_0/T as a function of H/H_{c2} for PdTe is plotted in Fig. 4, with $\kappa_{N0}(0.23\ \mathrm{T})/T = 7.86$ mW K^{-2} cm^{-1} and $\mu_0 H_{c2}(0) = 0.23$ T. For comparison, similar data of the clean s-wave superconductor Nb [35], the dirty s-wave superconducting alloy InBi [31], the multiband s-wave superconductor $NbSe_2$ [32] and $PbTaSe_2$ [36], and an overdoped d-wave cuprate superconductor $Tl_2Ba_2CuO_{6+\delta}$ (Tl-2201) [33] are also plotted.

In single-band clean s-wave superconductors, as well as in multiband s-wave superconductors as $T \to 0$ K, quasiparticles are localized within the vortex core, and conduction perpendicular to the magnetic field is predominantly attributed to the tunneling between adjacent vortices [26]. As the magnetic field increases, it becomes easier for quasiparticles to tunnel between vortex cores, leading to a slow exponential growth of κ_0/T versus H, as is indeed observed in Nb [35]. For dirty s-wave superconductor InBi, the response curve exhibits an exponential H dependence at low magnetic fields, while manifesting an approximately linear behavior as the magnetic field approaches H_{c2} [31]. For the nodal superconductor Tl-2201, a small field can yield a rapid growth due to the Volovik effect, and the low field $\kappa_0(H)/T$ shows roughly a $\sqrt{H}$ dependence [33]. In the case of multigap nodeless superconductors, the magnetic field dependence of $\kappa_0(H)/T$ relies on the ratio between the large and small gaps. For example, in the typical two-band superconductor $NbSe_2$, the ratio of different gap magnitudes is approximately 3 [32]. A rapid rise in low fields can be attributed to the fast suppression of the smaller gap by the applied field.

Figure 4 shows that the curve of the normalized $\kappa_0(H)/T$ for PdTe is very close to that of the multiband s-wave superconductor $PbTaSe_2$. Both of them are S-shaped curves [36]. Interestingly, nickel-based superconductors such as $BaNi_2As_2$, $TlNi_2Se_2$, and $SrNi_2P_2$ also exhibit S-shaped field dependence of $\kappa_0(H)/T$ curves [37–39]. Such an S-shaped $\kappa_0(H)/T$ curve is evidence for multiple nodeless superconducting gaps [36,38]. The low-field part is very flat, with absolute value close to zero, which means the gap(s) is quite isotropic, not highly anisotropic. The quite fast growth of κ_0/T above 20% H_{c2} very likely comes from the suppression of a smaller superconducting gap by the magnetic field. Indeed, the multiband electronic structure of PdTe has been demonstrated by density functional theory (DFT) calculations and de Haas–van Alphen (dHvA) oscillation experiments, and the superconducting specific heat can be well described with two nodeless energy gaps by using the two-band model to fit the data up to T_c [25].

While our ultra-low-temperature thermal-conductivity measurements clearly show multiple nodeless superconducting gaps in PdTe, previous ARPES measurements found that the bulk states near $\overline{Z}$ have a node in the superconducting state by exploring the bands close to the Brillouin zone boundary [24]. One of the most feasible explanations for this apparent discrepancy is that the ARPES measurements were only performed at 2 K (about 45% of the T_c), not low enough to observe the relatively smaller gap. In other words, the smallest gap among multiple superconducting gaps is still close at 2 K. This is supported by the exponential T dependence of C_e/T below 1.5 K, which suggests a fully open superconducting gap at very low temperature. Note that in Ref. [25], a residual linear term in specific heat $\gamma_r = 0.65$ mJ mol^{-1} K^{-2} was obtained by the fitting, which is attributed to nodal quasiparticles or a nonsuperconducting impure phase. In our specific heat data, the γ_r is smaller (0.31 mJ mol^{-1} K^{-2}). Since the absence of κ_0/T in zero field in Fig. 3(a) indicates that there is no gap node, such a small γ_r should be extrinsic.

Since the node previous ARPES measurements identified is a point node, another less possible explanation for the apparent discrepancy is that our heat flow is perpendicular to the nodal direction. In this case we may not be able to observe the κ_0/T in zero field contributed by the nodal quasiparticles. Limited by the small size and irregular shape of PdTe single crystals, during preparation of the rectangle sample, we are not able to determine the direction of the heat flow in it. The large surface of the rectangle sample is not a high-symmetry plane. Nevertheless, the chance for the heat flow to be perpendicular to the nodal direction should be very small. To further diminish this chance, we measured another sample and got similar thermal-conductivity results (not shown). More experiments at low temperature (at least down to 10% of the T_c), such as scanning tunneling microscopy (STM), muon spin relaxation (μSR), and ARPES, are needed to further clarify the superconducting gap structure in PdTe. Finally, we would like to point out that both PdTe and $PbTaSe_2$ are superconductors with multiple nodeless gaps and topological band structure, which makes them candidates for natural topological superconductors.

IV. SUMMARY

In summary, we have examined the superconducting gap structure of the topological Dirac semimetal PdTe through ultra-low-temperature thermal-conductivity measurements. The negligible κ_0/T at zero field and the S-shaped field dependence of $\kappa_0(H)/T$ demonstrate multiple nodeless superconducting gaps in PdTe. This is in contrast to the bulk-nodal gap claimed by previous ARPES measurements at 2 K. In this sense, the superconductivity in PdTe may not be unconventional, but it is still a good candidate for topological superconductors.

ACKNOWLEDGMENTS

We thank Rui Peng for helpful discussions. This work was supported by the Natural Science Foundation of China (Grant No. 12174064) and the Shanghai Municipal Science and Technology Major Project (Grant No. 2019SHZDZX01). Z.X. was supported by the Natural Science Foundation of China (Grant No. 12174334) and the National Key Projects for Research & Development of China (Grant No. 2019YFA0308602). Y.G. was supported by the open project of Beijing National Laboratory for Condensed Matter Physics (Grant No. ZBJ2106110017) and the Double First-Class Initiative Fund of ShanghaiTech University. X.X. was supported by the National Natural Science Foundation of China (Grants No. 12274369 and No. 11974061). D.D. and R.J. were supported by Grant No. DE-SC0024501 funded by the U.S. Department of Energy, Office of Science.

C.Z., X.L., and J.W. contributed equally to this work.

[1] M. R. Norman, The challenge of unconventional superconductivity, Science **332**, 196 (2011).

[2] X. L. Qi and S. C. Zhang, Topological insulators and superconductors, Rev. Mod. Phys. **83**, 1057 (2011).

[3] X. H. Chen, P. C. Dai, D. L. Feng, T. Xiang, and F. C. Zhang, Iron-based high transition temperature superconductors, Natl. Sci. Rev. **1**, 371 (2014).

[4] W. Liu, L. Cao, S. Zhu, L. Kong, G. Wang, M. Papaj, P. Zhang, Y.-B. Liu, H. Chen, G. Li, F. Yang, T. Kondo, S. Du, G.-H. Cao, S. Shin, L. Fu, Z. Yin, H.-J. Gao, and H. Ding, A new Majorana platform in an Fe-As bilayer superconductor, Nat. Commun. **11**, 5688 (2020).

[5] P. Zhang, K. Yaji, T. Hashimoto, Y. Ota, T. Kondo, K. Okazaki, Z. Wang, J. Wen, G. D. Gu, H. Ding, and S. Shin, Observation of topological superconductivity on the surface of an iron-based superconductor, Science **360**, 182 (2018).

[6] Q. Liu, C. Chen, T. Zhang, R. Peng, Y.-J. Yan, C.-H.-P. Wen, X. Lou, Y.-L. Huang, J.-P. Tian, X.-L. Dong, G.-W. Wang, W.-C. Bao, Q.-H. Wang, Z.-P. Yin, Z.-X. Zhao, and D.-L. Feng, Robust and clean Majorana zero mode in the vortex core of high-temperature superconductor $(Li_{0.84}Fe_{0.16})OHFeSe$, Phys. Rev. X **8**, 041056 (2018).

[7] C. Chen, Q. Liu, T. Z. Zhang, D. Li, P. P. Shen, X. L. Dong, Z.-X. Zhao, T. Zhang, and D. L. Feng, Quantized conductance of Majorana zero mode in the vortex of the topological superconductor $(Li_{0.84}Fe_{0.16})OHFeSe$, Chin. Phys. Lett. **36**, 057403 (2019).

[8] D. A. Ivanov, Non-Abelian statistics of half-quantum vortices in *p*-wave superconductors, Phys. Rev. Lett. **86**, 268 (2001).

[9] J. Ishizuka, S. Sumita, A. Daido, and Y. Yanase, Insulator-metal transition and topological superconductivity in UTe_2 from a first-principles calculation, Phys. Rev. Lett. **123**, 217001 (2019).

[10] I. M. Hayes, D. S. Wei, T. Metz, J. Zhang, Y. S. Eo, S. Ran, S. R. Saha, J. Collini, N. P. Butch, D. F. Agterberg, A. Kapitulnik, and J. Paglione, Multicomponent superconducting order parameter in UTe_2, Science **373**, 797 (2021).

[11] D. Aoki, H. Sakai, P. Opletal, Y. Tokiwa, J. Ishizuka, Y. Yanase, H. Harima, A. Nakamura, D. Li, Y. Homma, Y. Shimizu, G. Knebel, J. Flouquet, and Y. Haga, Core-level photoelectron spectroscopy study of UTe_2, J. Phys. Soc. Jpn. **91**, 083704 (2022).

[12] C. Broyles, Z. Rehfuss, H. Siddiquee, J. A. Zhu, K. Zheng, M. Nikolo, D. Graf, J. Singleton, and S. Ran, Revealing a 3D Fermi surface pocket and electron-hole tunneling in UTe_2 with quantum oscillations, Phys. Rev. Lett. **131**, 036501 (2023).

[13] S. Sasaki, M. Kriener, K. Segawa, K. Yada, Y. Tanaka, M. Sato, and Y. Ando, Topological superconductivity in $Cu_xBi_2Se_3$, Phys. Rev. Lett. **107**, 217001 (2011).

[14] J. X. Yin, Z. Wu, J. H. Wang, Z. Y. Ye, J. Gong, X. Y. Hou, L. Shan, A. Li, X. J. Liang, X. X. Wu, J. Li, C. S. Ting, Z. Q. Wang, J. P. Hu, P. H. Hor, H. Ding, and S. H. Pan, Observation of a robust zero-energy bound state in iron-based superconductor Fe(Te, Se), Nat. Phys. **11**, 543 (2015).

[15] P. Zhang, Z. Wang, X. Wu, K. Yaji, Y. Ishida, Y. Kohama, G. Dai, Y. Sun, C. Bareille, K. Kuroda, T. Kondo, K. Okazaki, K. Kindo, X. Wang, C. Jin, J. Hu, R. Thomale, K. Sumida, S. Wu, K. Miyamoto *et al.*, Multiple topological states in iron-based superconductors, Nat. Phys. **15**, 41 (2019).

[16] Y. Fang, J. Pan, D. Zhang, D. Wang, H. T. Hirose, T. Terashima, S. Uji, Y. Yuan, W. Li, Z. Tian, J. Xue, Y. Ma, W. Zhao, Q. Xue, G. Mu, H. Zhang, and F. Huang, Discovery of superconductivity in 2M WS_2 with possible topological surface states, Adv. Mater. **31**, 1901942 (2019).

[17] Y. Yuan, J. Pan, X. Wang, Y. Fang, C. Song, L. Wang, K. He, X. Ma, H. Zhang, F. Huang, W. Li, and Q.-K. Xue, Evidence of anisotropic Majorana bound states in 2M-WS_2, Nat. Phys. **15**, 1046 (2019).

[18] A. B. Karki, D. A. Browne, S. Stadler, J. Li and R. Jin, PdTe: A strongly coupled superconductor, J. Phys.: Condens. Matter **24**, 055701 (2012).

[19] A. B. Karki, V. O. Garlea, R. Custelcean, S. Stadler, E. W. Plummer, and R. Jin, Interplay between superconductivity and magnetism in $Fe_{1-x}Pd_xTe$, Proc. Natl. Acad. Sci. USA **110**, 9283 (2013).

[20] B. Tiwari, R. Goyal, R. Jha, A. Dixit, and V. P. S Awana, PdTe: A 4.5 K type II BCS superconductor, Supercond. Sci. Technol. **28**, 055008 (2015).

[21] C. E. Ekuma, C.-H. Lin, J. Moreno, W. Ku, and M. Jarrell, First-principles Wannier function analysis of the electronic structure of PdTe: weaker magnetism and superconductivity, J. Phys.: Condens. Matter **25**, 405601 (2013).

[22] J.-J. Cao and X.-F. Gou, First-principles study of electronic structure, phonons and electron-phonon interactionin hexagonal PdTe, Physica C: Supercond. Appl. **520**, 19 (2016).

[23] J. Chen and X. Wang, Superconductivity origin of PdTe and pressure effect: Insights from first-principles investigation, Solid State Sci. **52**, 23 (2016).

[24] X. P. Yang, Y. Zhong, S. Mardanya, T. A. Cochran, R. Chapai, A. Mine, J. Zhang, J. Sánchez-Barriga, Z.-J. Cheng, O. J. Clark, J.-X. Yin, J. Blawat, G. Cheng, I. Belopolski, T. Nagashima, S. Najafzadeh, S. Gao, N. Yao, A. Bansil, R. Jin, T.-R. Chang, S. Shin, K. Okazaki, and M. Zahid Hasan, Coexistence of bulk-nodal and surface-nodeless Cooper pairings in a superconducting Dirac semimetal, Phys. Rev. Lett. **130**, 046402 (2023).

[25] R. Chapai, P. V. S. Reddy, L. Xing, D. E. Graf, A. B. Karki, T.-R. Chang, and R. Jin, Evidence for unconventional superconductivity and nontrivial topology in PdTe, Sci. Rep. **13**, 6824 (2023).

[26] H. Shakeripour, C. Petrovic, and L. Taillefer, Heat transport as a probe of superconducting gap structure, New J. Phys. **11**, 055065 (2009).

[27] J. A. Woollam, P. B. Somoano, and P. O. Connor, Positive curvature of the H_{c2}-versus-T_2 boundaries in layered superconductor, Phys. Rev. Lett. **32**, 712 (1974).

[28] C. K. Jones, J. K. Hulm, and B. S. Chandrasekhar, Upper critical field of solid solution alloys of the transition element, Rev. Mod. Phys. **36**, 74 (1964).

[29] S. Y. Li, J.-B. Bonnemaison, A. Payeur, P. Fournier, C. H. Wang, X. H. Chen, and L. Taillefer, Low-temperature phonon thermal conductivity of single-crystalline Nd_2CuO_4: Effects of sample size and surface roughness, Phys. Rev. B **77**, 134501 (2008).

[30] M. Sutherland, D. G. Hawthorn, R. W. Hill, F. Ronning, S. Wakimoto, H. Zhang, C. Proust, E. Boaknin, C. Lupien, L. Taillefer, R. Liang, D. A. Bonn, W. N. Hardy, R. Gagnon, N. E. Hussey, T. Kimura, M. Nohara, and H. Takagi, Thermal conductivity across the phase diagram of cuprates: Low-energy quasiparticles and doping dependence of the superconducting gap, Phys. Rev. B **67**, 174520 (2003).

[31] J. O. Willis and D. M. Ginsberg, Thermal conductivity of superconducting alloy films in a perpendicular magnetic field, Phys. Rev. B **14**, 1916 (1976).

[32] E. Boaknin, M. A. Tanatar, J. Paglione, D. Hawthorn, F. Ronning, R. W. Hill, M. Sutherland, L. Taillefer, J. Sonier, S. M. Hayden, and J. W. Brill, Heat conduction in the vortex state of $NbSe_2$: Evidence for multiband superconductivity, Phys. Rev. Lett. **90**, 117003 (2003).

[33] C. Proust, E. Boaknin, R. W. Hill, L. Taillefer, and A. P. Mackenzie, Heat transport in a strongly overdoped cuprate: Fermi liquid and a pure d-wave BCS superconductor, Phys. Rev. Lett. **89**, 147003 (2002).

[34] E. Boaknin, Thermal conductivity in the vortex state of unconventional superconductors, Ph.D. thesis, University of Toronto, 2003.

[35] J. Lowell and J. B. Sousa, Mixed-state thermal conductivity of type II superconductors, J. Low Temp. Phys. **3**, 65 (1970).

[36] M. X. Wang, Y. Xu, L. P. He, J. Zhang, X. C. Hong, P. L. Cai, Z. B. Wang, J. K. Dong, and S. Y. Li, Nodeless superconducting gaps in noncentrosymmetric superconductor $PbTaSe_2$ with topological bulk nodal lines, Phys. Rev. B **93**, 020503(R) (2016).

[37] N. Kurita, F. Ronning, Y. Tokiwa, E. D. Bauer, A. Subedi, D. J. Singh, J. D. Thompson, and R. Movshovich, Low-temperature magnetothermal transport investigation of a Ni-based superconductor $BaNi_2As_2$: Evidence for fully gapped superconductivity, Phys. Rev. Lett. **102**, 147004 (2009).

[38] X. C. Hong, Z. Zhang, S. Y. Zhou, J. Pan, Y. Xu, H. D. Wang, Q. H. Mao, M. H. Fang, J. K. Dong, and S. Y. Li, Multigap nodeless superconductivity in nickel chalcogenide $TlNi_2Se_2$, Phys. Rev. B **90**, 060504(R) (2014).

[39] N. Kurita, F. Ronning, C. F. Miclea, E. D. Bauer, K. Gofryk, J. D. Thompson, and R. Movshovich, Fully gapped superconductivity in $SrNi_2P_2$, Phys. Rev. B **83**, 094527 (2011).